Advanced Energy Conversion Materials
http://ojs.wiserpub.com/index.php/AECM/

UNIVERSAL WISER PUBLISHER

Research Article

# Synthesis and Performance Elucidation of Ternary O3-$Na_{0.8}Fe_{0.4}Mn_{0.3}Co_{0.2}O_2$ Layered Positive Electrode for Sodium Ion Batteries

**M. Alam Khan[1*], Sunil Singh[2]**

[1]Department of Energy and Materials Engineering, Dongguk University-Seoul, Seoul 100-715, Republic of Korea
[2]Vivekananda College of Technology, Mathura Bypass, Gonda Road, Aligarh, 202002, U.P. India
E-mail: alamkhan77@gmail.com

**Received:** 30 September 2021; **Revised:** 15 November 2021; **Accepted:** 23 November 2021

**Abstract:** We report here a combination of transition metal-based ternary sodium magnate layered cathodes with the compositions of $Na_{0.8}Fe_{0.4}Mn_{0.3}Co_{0.2}O_2$, $Na_{0.8}Fe_{0.4}Mn_{0.3}Ni_{0.2}O_2$, $Na_{0.8}Fe_{0.4}Mn_{0.3}V_{0.2}O_2$, $Na_{0.8}Fe_{0.4}Mn_{0.3}Ti_{0.2}O_2$, in order to elucidate the precise metal contents for the superb performing positive electrode. Based on their stoichiometry, the transition metal combination of $Na_{0.8}Fe_{0.4}Mn_{0.3}Co_{0.2}O_2$, O3-type crystal structure with R3m space group possess superior electrochemical behavior under the test of sodium-ion battery. When the charge-discharge capacities in the range of 2.0-4.2 V at 0.1 C are measured, it shows the comparatively higher performance of the first and second charge capacities of 162 $mAhg^{-1}$, 170 $mAhg^{-1}$ and discharge capacities of 157 $mAhg^{-1}$, 154 $mAhg^{-1}$, respectively. Moreover, it was remarkable to observe that the increasing/decreasing Co constituent substantially affects the performance and stability, but using the ternary combination in cathodes, a substantial reduction of Jahn-Teller distortion and increased biphasic characteristics were observed. The as-synthesized samples were characterized by FE-SEM, XRD, charge-discharge curve, EIS and cyclic voltammograms.

***Keywords*:** ternary O3-type cathodes, XRD, layered structure, sodium-ion batteries, solid-state reaction

## 1. Introduction

Since the first successful commercialization of lithium-ion battery in 1991 by Sony incorporation [1], concomitantly, the astounding demand for energy in mobile lightweight items rapidly opens avenues to investigate new energy storage technologies such as Ni-Cd, Ni-Metal hydride for electric vehicles. Moreover, today's life deals with the myriad portable electronic gadgets that require smaller but powerful energy storage systems [2]. Additionally, over the past two decades with the continuous surging thirst for large-scale energy storage systems for electric vehicles and the energy grid systems, the concern about the depletion of lithium reservoirs has been getting greater apprehensions [3-4]. On the other hand, the pressing environmental concern and greenhouse gas generation from burning fossil fuels to quench current energy demand for steeping world population shifts the paradigm for alternative energy sources with an abundant supply of material constituents [5]. Among all the formidable options, sodium-ion battery with extreme cost-effectiveness, abundance and wide geographical distribution is a highly promising alternative energy-storage candidate for sustainable future energy demands [6-7].

Consequently, sodium with the 4$^{th}$ most abundant element in earth crust (28400 mg/kg compared to Li, 20 mg/kg), the


DOI: https://doi.org/10.37256/aecm.3120221187

second lightest in alkali metal family, second in size 1.02Å (Li = 0.76Å) and with standard electrode potential of -2.71 V vs SHE (Li-3.04 V vs SHE), have similar battery chemistry and could enable sodium for lithium substitution lowering the cost of almost 30 times when utilized in the devices [8-9]. However, the large ionic radius of sodium ion (0.95 nm) compared to lithium-ion (0.60 nm) has a lower insertion in the three-dimensional (3D) material interfaces such as spinel compounds. Thus, the layered structures with larger inter-slab distances allow the readily insertion of larger ionic sized metal both in and out of the crystalline structure. Mostly, the layered oxides of $Na_xMO_2$ (M: transition metal) with O3 or P2 phases (O: octahedral; P: prismatic) composed of repeating units of $MO_6$ layers with Na ions being sandwiched in the oxide layers are highly promising as cathode materials in sodium-ion batteries [10]. Remarkably, in the case of layered sodium metal oxides, the O3-phase mainly occurs when sodium constituent $0.7 < x < 1$, with sodium sharing on edges acquiring oxide layer stacking of ABCABC pattern [11]. While, P2-phase formed when $x < 0.7$, with Na shares either entire edge or entire face oxide layer with stacking of ABBA pattern, the ensuing electrochemical properties in each material are mostly influenced by the structure of phases, layer stability and kinetics effects of the surrounding atmosphere near sodium. So, various methodologies and strategies have been employed to synthesize and investigate the electrochemical, stability and reversible phase transformation in these layered oxide materials, providing many new insights and novel design of chemical compositions of metals that are possibly used for the high performance and stable sodium cathodes [12-13]. Practically, in the initial stages, a single transition metal layered oxides ($Na_xMO_2$) was reported where strong $Na^+$/vacancy interactions result in a stair-like multiple structural transition pattern upon cycling [14]. Recently layered spinel (P2/P3) multiphase/stair-like charge-discharge potential curve has also been reported [15] and perceived as unsuitable for the commercial purpose. Thus, the Fe substitution was carried out to avoid cation stabilization and reduced to the bi-phasic reaction following the report of Yabuuchi et al. (P2-$Na_xFe_{0.5}Mn_{0.5}O_2$), where many plateaus/stairs as observed in the case of $Na_xMnO_2$ were successfully eliminated. It delivered 190 $mAhg^{-1}$, thereby enabling the use of earth-abundant elements in cathode material for charge-discharge curve studies. However, it exhibited poor cycle retention of only 79% over the course of 30 cycles. Apparently the employed Fe substitution also appeared to increase the average voltage, suppressing Jahn-Teller distortion and improving capability substantially [16]. Komaba et al. realized that the intrinsic problem of structural instability was caused by the Fe-ion migration during the cycling process in the O3-type $NaFeO_2$ layer structure [17]. Later, this bottleneck was rectified by replacing the transition metal atoms in $TMO_2$ slabs to form the binary or ternary compounds such as $NaCo_xFeO_2$, $Na[Fe_x(Ni_{0.5}Mn_{0.5})_{1-x}]O_2$, and $Na[Li_{0.05}(Ni_{0.25}Fe_{0.25}Mn_{0.5})_{0.95}]O_2$ [18-20]. It has been further demonstrated that the substitution of iron to nickel in P2-$Na_{0.67}Ni_xFe_{0.35-x}Mn_{0.65}O_2$ ($x = 0, 0.15$) has improved the capacity and cyclability [21] and the P2 + O3 layered composite $Na_{0.66}Ni_{0.21}Mn_{0.71}Co_{0.08}Li_{0.18}O_{2+\delta}$ exhibits both good capacity and rate capability (185 $mAhg^{-1}$ at 20 $mAg^{-1}$, 134 $mAhg^{-1}$ at 100 $mAg^{-1}$ under the 1.5-4.5V vs $Na^+$/Na). The better electrochemical performance was ascribed to the P2 + O3 mixed crystal structure where higher capacity is given by O3 component and the enlargement of octahedral slab is due to P2 channels [22]. Moreover, in our recent study, we have demonstrated that mixed P2/O3 phases have dominant $Mn^{4+}$ ion which is ascribed to lower the Jahn-Teller distortion and performs well as cathode, even it contains a single transition metal ($Na_{0.8}Mn_{0.5}O_2$) in Na ion batteries (SIBs) [23]. Additionally, the well-known ternary O3-type $Na[Ni_xCo_yMn_z]O_2$ cathodes has been extensively studied in sodium-ion battery. Though the cobalt metal contributes well to the structural stability and rate capability, still they face capacity and cycling limitations due to their inherent structural instability due to high reactive $Ni^{4+}$ ions [24]. More often, it has been shown that Fe-rich O3-type cathodes have high discharge capacity but low rate capability and are researched extensively as rectifying of Jahn-Teller distortion since $Fe^{3+/4+}$ ion is low Jahn-Teller active [25]. Such intensive research efforts for cheap and abundant transition metal utilization have made great progress in capacity, rate capability and cycling stability and in the current scenario, they are still far behind the required successful application of rechargeable SIBs.

Since the design of a multi-mixture constituent of electrochemically active transition metals can selectively activate the redox properties and improve the quality of each desired element at a certain target voltage or may enhance cathode performance. So, a careful scheme could enable smooth charge-discharge profiles in order to avoid distortion or multi-phase transitions, tuning voltage, reduction in Jahn-Teller distortion, employing the inactive transition metals to stabilize the crystal structures to obtain promising stable cathodes for electrochemical performances. For example, the substitution of cobalt for nickel to form $Na_{0.7}Mn_{0.7}$-$Ni_{0.3x}Co_xO_2$ ($x = 0, 0.1, 0.3$) has improved the electrochemical performance by (a) enlarging the d-space of inter-slab, improving sodium-ion diffusion, while (b) shrinking TM-O and O-O bond lengths to improve structural stability, and (c) enhancing electronic conductivity [26]. Similarly,

cathode material of O3-$Na_{0.9}Mn_{0.4}Fe_{0.5}Ti_{0.1}O_2$ was found to possess a capacity of 197 $mAhg^{-1}$ when cycled between 1.5-4.2 V at 0.1 C, though this rapidly fell to 167 $mAhg^{-1}$ by the 3rd cycle and 100 by the 40$^{th}$ [27]. Considering all the merits of transition metals, herein, we report a high-performance O3-type ternary transition metal layered oxide with $Na_{0.8}Fe_{0.4}Mn_{0.3}Co_{0.2}O_2$ composition as a new cathode material.

## 2. Experimental section

*Sample Synthesis:* The samples containing various amounts of sodium, iron, cobalt, nickel, vanadium, titanium and manganese metals for the synthesis of O3-phase layered oxide use a solid-state reaction method to maintain the stoichiometric amount of precursor sources as $Na_2CO_3$ (Aldrich), $Fe_2O_3$ (Aldrich), $V_2O_5$ (Aldrich), $TiO_2$ (Aldrich), CoO (Aldrich), NiO (Aldrich) and $Mn_2O_3$ (Aldrich) at 700 °C for 10 h in the continuous airflow of 1 $ml/cm^3$ in the tubular furnace (Daesung Co., Ltd). The ratios of Na:Fe:Mn:Co were maintained as 0.8:0.4:0.3:0.2 in the best sample and other samples transition metals (Ni, V, Ti, Mn, Fe) in the same composition were maintained. And it was first ball milled (FRITSCH, Pulverisette) in acetone solvent at 300 rpm/min for the 3 h, then dried and made as thin pellets using 0.4 g sample that was pressed manually. The obtained samples were then placed in the tube furnace and after reaction immediately taken and placed in the glove box. The pellets were then powdered by using mortar before the slurry fabrication, for the electrochemical and other characterization studies the sample was kept respectively in argon-filled glove box in the sealed vials.

*Characterizations of prepared samples:* The crystal structures of the synthesized samples (other compositions) were characterized by powder X-ray diffraction (Rigaku XRD-6000 Cu-Kα radiation, l51.5418 Å). The diffraction data were scanned at the rate of 2°/min in the 2θ range of 10-70°. The nanoparticle's morphology details were analyzed by a scanning electron microscope (FE-SEM) (S-4300 Shimadzu, 15 kV) and EDX spectra for element mappings. The cyclic voltammetry (CV) was also applied with a scan rate of 0.1 mV between 2.0 and 4.2 V vs. $Na/Na^+$ by the Wonatech WBCS 3000 system (Korea).

*Electrochemical analysis:* The electrochemical performance studies of cycling tests were performed by fabricating coin cells (CR-2032) in the glove box. First, the electrode slurries were prepared by a mixture of active materials with various compositions with acetylene black and polyvinylidene fluoride (PVDF) in the weight ratio of 80:10:10 with some additional drops of N-methyl-2-pyrrolidone (NMP) were pasted by doctor blade technique on the aluminum foil which was dried at 120 °C for 5h in the vacuumed oven before the cell assembling. A half-cell was assembled using the prepared electrode as a cathode, a piece of separator (Celgard 2500), pure Na ingots for foil as cathode, and electrolyte (1 M $NaPF_6$ in EC: DEC organic solutions) were utilized under the glove box. Similarly, all the other transition metals stoichiometry containing combinations were made separately from the same procedure for the sodium half cells and analyzed. The TOSCAT 3000 U (Toyosystem Co., Ltd) battery tester was used to perform the galvanic charge and discharge testing in which all of the prepared samples were conducted in a voltage range of 2.0-4.2 V vs. $Na/Na^+$ (0.1 C) at ambient.

## 3. Results and discussion

The powder X-ray diffraction (XRD) patterns of as-synthesized ternary compounds using a stoichiometric amount of transition metals (Fe, Mn, Ni, Co, V, Ti) are presented in Figure 1. The basic observed pattern in all those samples has similarity in the 2 theta positions, but the sample $Na_{0.8}Fe_{0.4}Mn_{0.3}V_{0.2}O_2$ has remarkable high intensity peaks. In general, all the peaks in $Na_{0.8}Fe_{0.4}Mn_{0.3}Ni_{0.2}O_2$, $Na_{0.8}Fe_{0.4}Mn_{0.3}V_{0.2}O_2$, $Na_{0.8}Fe_{0.4}Mn_{0.3}Co_{0.2}O_2$, $Na_{0.8}Fe_{0.4}Mn_{0.3}Ti_{0.2}O_2$ samples can be indexed as rhombohedral O3-type crystal structure with space group R3m ($a_{hex}$ = 2.9637Å; $c_{hex}$ = 16.222 Å), and they mostly match with the referenced ICSD85825 and are indexed as 2θ position of 15.8º, 32.0º, 35.2º, 39.0º, 41.5º, 43.0º, 48.9º, 52.9º, 62.6º, 64.8º, 67.0º corresponding to (003), (006), (101), (102), (104), (105), (009), (107), (110), (1010), (113) crystal phases [28]. However, (003) peak in the ternary sample of $Na_{0.8}Fe_{0.4}Mn_{0.3}Ni_{0.2}O_2$ slightly (0.15 degrees) shifted to higher theta values. More significant difference observed in the peak intensities containing vanadium with a few new peaks by considering differences to other samples in the range of 2theta 30°-48°, the high intense 41.5° peak completely absent or a tiny peak was observed in all as it behaves more like a mixed O3/P2 with a dominant tendency of P2 crystal

structure exhibiting four dominant Bragg diffraction peaks with a slight variant in the intensities at 33° (004), 35.5° (100), 37.0° (102) and 40.9° (103). However, it also possesses peak positions of O3 phases at 31.5° (006), 38.9° (102) in those ranges clarifying a mixed tendency. Two other new peaks at 2θ positions of 49.5° and 54.0° are also found in the vanadium-containing samples only. The difference in vanadium-containing material from the rest of the samples arises even the same experimental protocol for synthesis was employed. It has been reported that it is quite difficult to obtain a single $Na_xVO_2$ phase without impurity due to possible phase conversion between $O_2$ and $V^{3+}$ with high reducing activity [28-29], perhaps in our sample similar behavior were observed as reported elsewhere. The observed results from all other samples could be inferred, as Mn tends to lower the crystallinity while Fe enhances this tendency which may give us clues about better electron transport in iron-containing samples. Nevertheless, it has been found that all the samples possess a dominant tendency towards O3-type phase crystal structures [28].

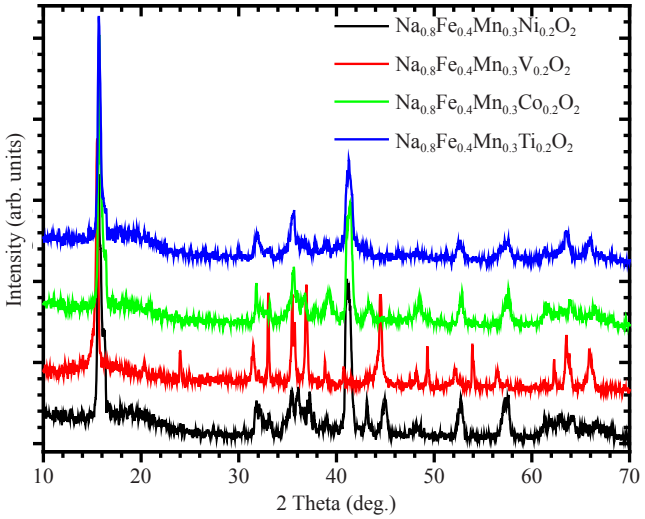


**Figure 1.** X-ray diffraction patterns of the synthesized samples containing O3-type crystal structure with different ternary compositions.

The galvanostatic performance of charge-discharge curve of $Na_{0.8}Fe_{0.4}Mn_{0.3}Ni_{0.2}O_2$, $Na_{0.8}Fe_{0.4}Mn_{0.3}V_{0.2}O_2$, $Na_{0.8}Fe_{0.4}Mn_{0.3}Co_{0.2}O_2$, $Na_{0.8}Fe_{0.4}Mn_{0.3}Ti_{0.2}O_2$ ternary samples with the stoichiometric composition of transition metals (Fe, Mn, Ni, Co, V, Ti) which were analyzed at 2.0 to 4.2 V with a current density of 0.1 C are presented in Figure 2(a). Each of the corresponding Figure 2(b) represents respective cycle stability with metal constituent composition mentioned inside of each figures. It is clearly observed that samples with different transition metal combinations show very different and interesting performances based solely on the type of ternary metal content (Ni, Co, V, Ti) ratios such as $Ni_{0.2}$ content showing the first and second charge capacities of 147 $mAhg^{-1}$, 131 $mAhg^{-1}$ and the discharge capacities of 124 $mAhg^{-1}$, 117 $mAhg^{-1}$ and vanadium-based $Na_{0.8}Fe_{0.4}Mn_{0.3}V_{0.2}O_2$ cathode shows 67 $mAhg^{-1}$, 88 $mAhg^{-1}$ with discharge capacities of 84 $mAhg^{-1}$, 85 $mAhg^{-1}$ while the cobalt-containing cathode sample of $Na_{0.8}Fe_{0.4}Mn_{0.3}Co_{0.2}O_2$ shows the first and second charge capacities a remarkable 162 $mAhg^{-1}$, 170 $mAhg^{-1}$ and discharge capacities of 157 $mAhg^{-1}$, 154 $mAhg^{-1}$ and the titanium-based cathode sample of $Na_{0.8}Fe_{0.4}Mn_{0.3}Ti_{0.2}O_2$ shows capacities of 153 $mAhg^{-1}$, 145 $mAhg^{-1}$ and discharge capacities of 136 $mAhg^{-1}$, 127 $mAhg^{-1}$, respectively. Overall, the best electrochemical performance with the cobalt ($Na_{0.8}Fe_{0.4}Mn_{0.3}Co_{0.2}O_2$) composition was observed compared to other transition-based samples that also show superior capacity retention of ~82.2%. The explored combinations here for the search of better cathode material were speculated based on the trade-off of electrochemical performances, biphasic stability and reduced Jahn-Teller distortion that might be well rectifying, thus resulting in a better efficiency. Furthermore, the stability and longer retention time along with Coulombic efficiency characteristics were measured in sodium-ion batteries which are reported in Figure 2(b). The results depicted a stable cyclic capacity up to 90 cycles in the best sample ($Na_{0.8}Fe_{0.4}Mn_{0.3}Co_{0.2}O_2$) having an average of 98.5% of Coulombic efficiency, the specific discharge capacity of 2$^{nd}$ (154.1 $mAg^{-1}$) and 85$^{th}$ (126.8 $mAg^{-1}$) cycle in the best sample exhibits capacity retention of 82.3%.

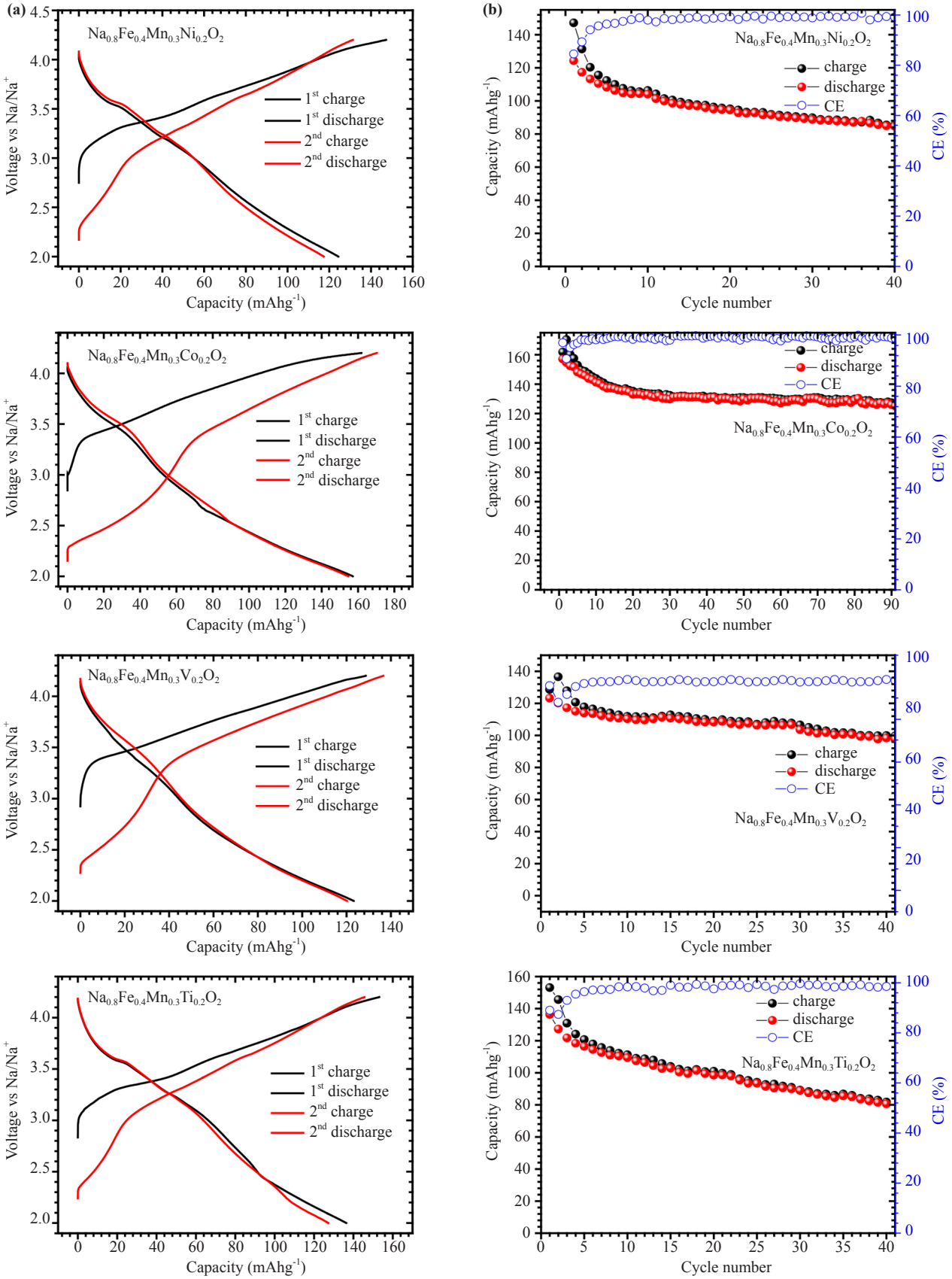


**Figure 2.** Galvanostatic voltage profiles of the synthesized samples containing O3-type crystal structure with different ternary compositions (a). Corresponding cycle stability and Coulombic efficiency graphs (b).

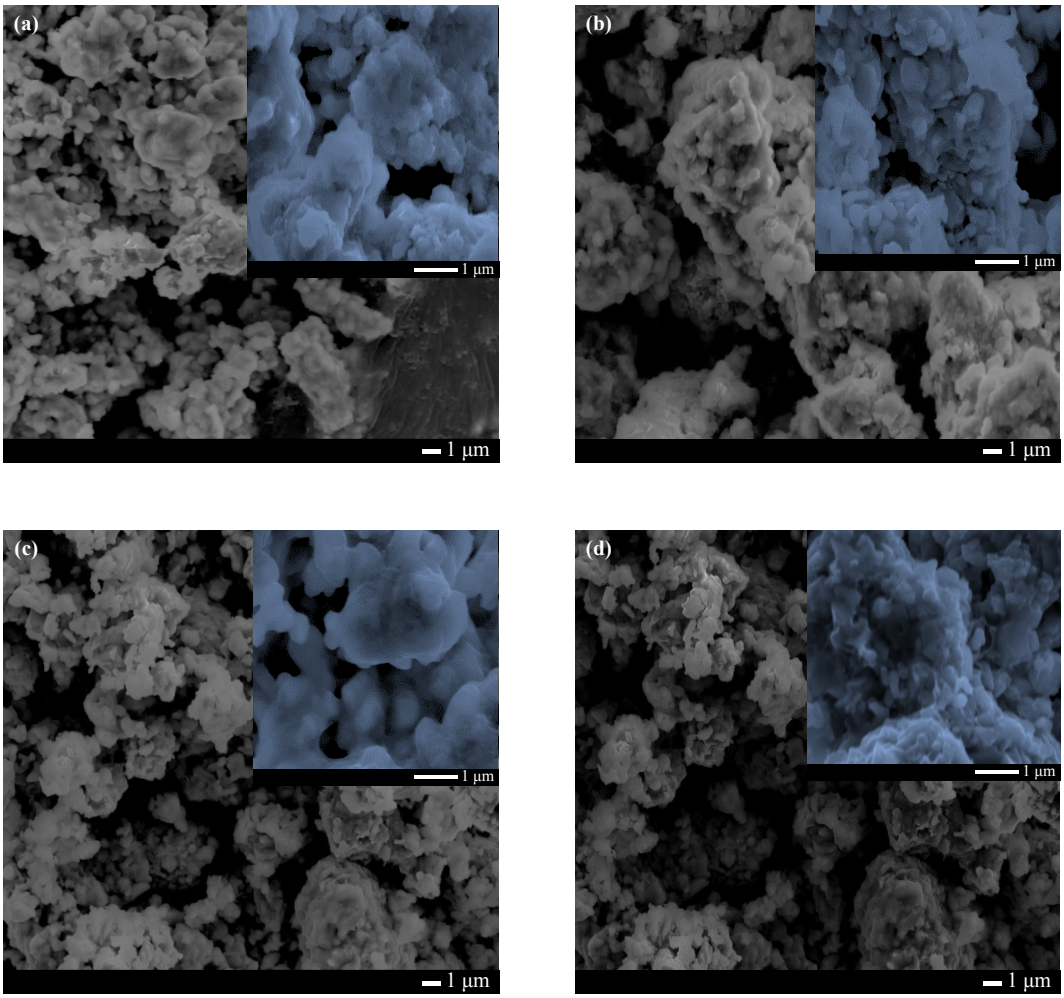


**Figure 3.** FE-SEM analysis of synthesized samples containing $Na_{0.8}Fe_{0.4}Mn_{0.3}Ni_{0.2}O_2$ (a), $Na_{0.9}Fe_{0.4}Mn_{0.3}Co_{0.2}O_2$ (b), $Na_{0.8}Fe_{0.4}Mn_{0.3}V_{0.2}O_2$ (c), $Na_{0.8}Fe_{0.4}Mn_{0.3}Ti_{0.2}O_2$ (d) as cathode materials.

In order to get more insight and visualize the change in local structures, phase transitions and sodium vacancy ordering are responsible for the smooth voltage plateaus. Figure 3(a-d) shows the morphological feature of the as-synthesized $Na_{0.8}Fe_{0.4}Mn_{0.3}Ni_{0.2}O_2$, $Na_{0.8}Fe_{0.4}Mn_{0.3}V_{0.2}O_2$, $Na_{0.8}Fe_{0.4}Mn_{0.3}Co_{0.2}O_2$, $Na_{0.8}Fe_{0.4}Mn_{0.3}Ti_{0.2}O_2$ nanocrystals are analyzed by the field emission scanning electron microscopy (FE-SEM). It has been observed that the smaller disc shape morphology in all samples possesses well-defined crystals typical to the layered structures and some of the crystals were also found agglomerated or fused with each other by a topotactic effect of the solid-state reaction conditions with a multi-size of the crystals forming a series of planes with an average size of ~500 nm to 1 µm in diameters which are more prominent with clear planes. Although it is hard to get many clear differences between the samples by the FE-SEM micrographs as visually observed more particle separation in the best sample was observed while in other samples particles were attached to the parent larger particles. The FE-SEM energy-dispersive X-ray spectroscopy (EDX) mapping of elements in our best sample is presented in Figure 4 where it is found to be a ternary elemental composition of Sodium, Iron, Manganese and Cobalt (Na:Fe:Mn:Co = 0.78:0.38:0.29:0.19) which matches well with the as-synthesized sample constituents. Figure 5(a-d) depicts the cyclic voltammetry (CV) analysis graphs of the corresponding samples in the sodium half cells at a sweep rate of $0.1mVs^{-1}$ in view to understand the electrochemical behavior for the first two cycles. The CV results depicted typical peaks associated with electrochemical sodium (de)-intercalation process into the O3-layered structure, involving reversible processes in the 2.0-4.2 V potential region with a series of anodic peaks at 2.4 V (shoulder), 2.73 V (broad peak), and 3.7 V while cathode peaks were 2.2 V, and 3.6 V, respectively. It

has been reported that anodic/cathode peaks at 2.6/1.9 V are caused by $Mn^{3+}/Mn^{4+}$ redox reactions and in our case, slight higher positions were observed that are ascribed to the Fe substitution. The intensity of the peaks does not have many differences in successive cycle speculating low polarization, phase change or irreversible structure variations on charging. Two dominant pairs of peaks are observed in both the anodic and cathode sweeps at 2.73 vs 2.2 V and 3.7 vs 3.6 V, corresponding to redox reactions of $Mn^{3+}/Mn^{4+}$ and $Fe^{3+}/Fe^{4+}$, respectively [30-31]. The higher anodic/cathode peak (1.73V/2.2V) may result from the higher Fe content and increased participation along with $Mn^{3+}/Mn^{4+}$ redox couple in the overall as a complex electrochemical delithiation/lithiation processes. Shoulders in the anodic peak at 2.06 V and 2.45 V are languishing in the second cycle which could be attributed to side reactions in the first cycle. The intensity of the peaks does not have much difference and overlaps well speculating of low polarization in our synthesized samples. The voltage plateaus associated with phase transitions are in good agreement with the corresponding charge-discharge curves in Figure 2. It is also interesting to point out that other samples (c, d) possess similar shapes of CV profiles compared to the corresponding anodic/cathode reactions which may imply similar mechanisms of $Na^+$ transportation, however, the excess of $Fe^{3+}$ effects on the performance is still not clear because of the complexity of the reactions at the current stage and detail study is going on. We ascribe that the larger quantity of $Fe^{3+}$ constituent leads to a strong interaction between Mn-O bonds with better stabilization of vacancy ordering by a partial excess amount of Fe substitution to Mn which results in a biphasic reaction as observed in Figure 2. It is considered that the intercalation and the de-intercalation reaction of Na result in the occurrence of peaks at voltages between 2.0 and 3.8 V. The elecrtrochemical impedance spectra (EIS) analysis presented in Figure 5(e) shows sample $Na_{0.8}Fe_{0.4}Mn_{0.3}Co_{0.2}O_2$, the charge transfer resistance ($R_{CT}$) possess semicircle arc which is smaller than other samples suggesting improved charge transfer speed and fast $Na^+$ ion diffusion through the electrolyte-electrode interface in the best sample are well consistent with the electrochemical performance as observed in Figure 2.

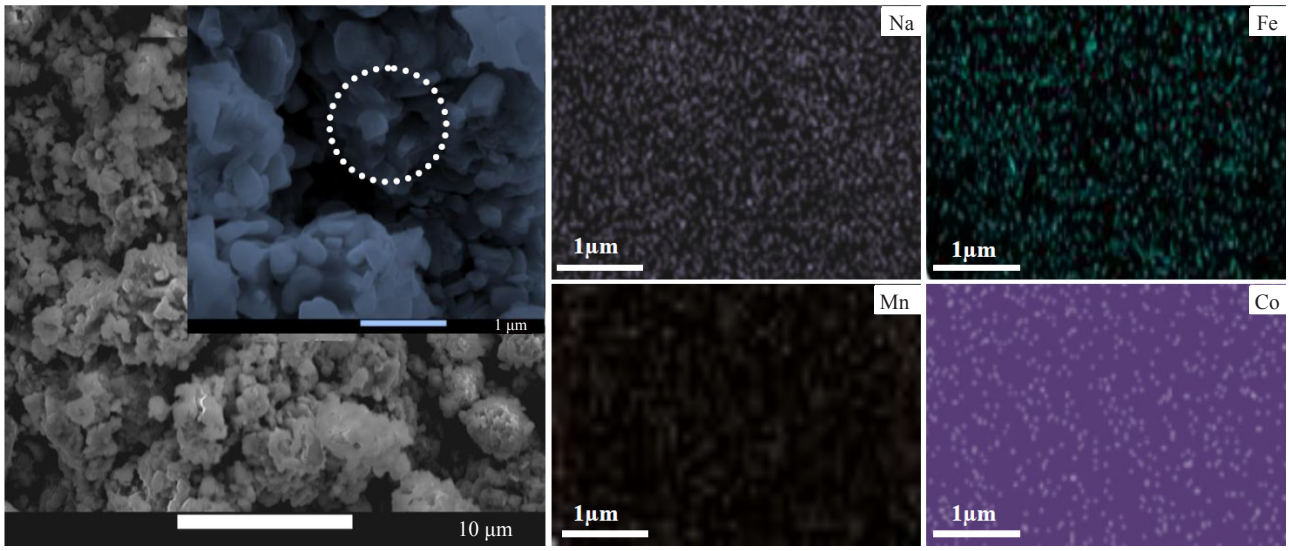


**Figure 4.** FE-SEM EDX elemental mapping analysis of the best synthesized sample ($Na_{0.9}Fe_{0.4}Mn_{0.3}Co_{0.2}O_2$) as cathode material.

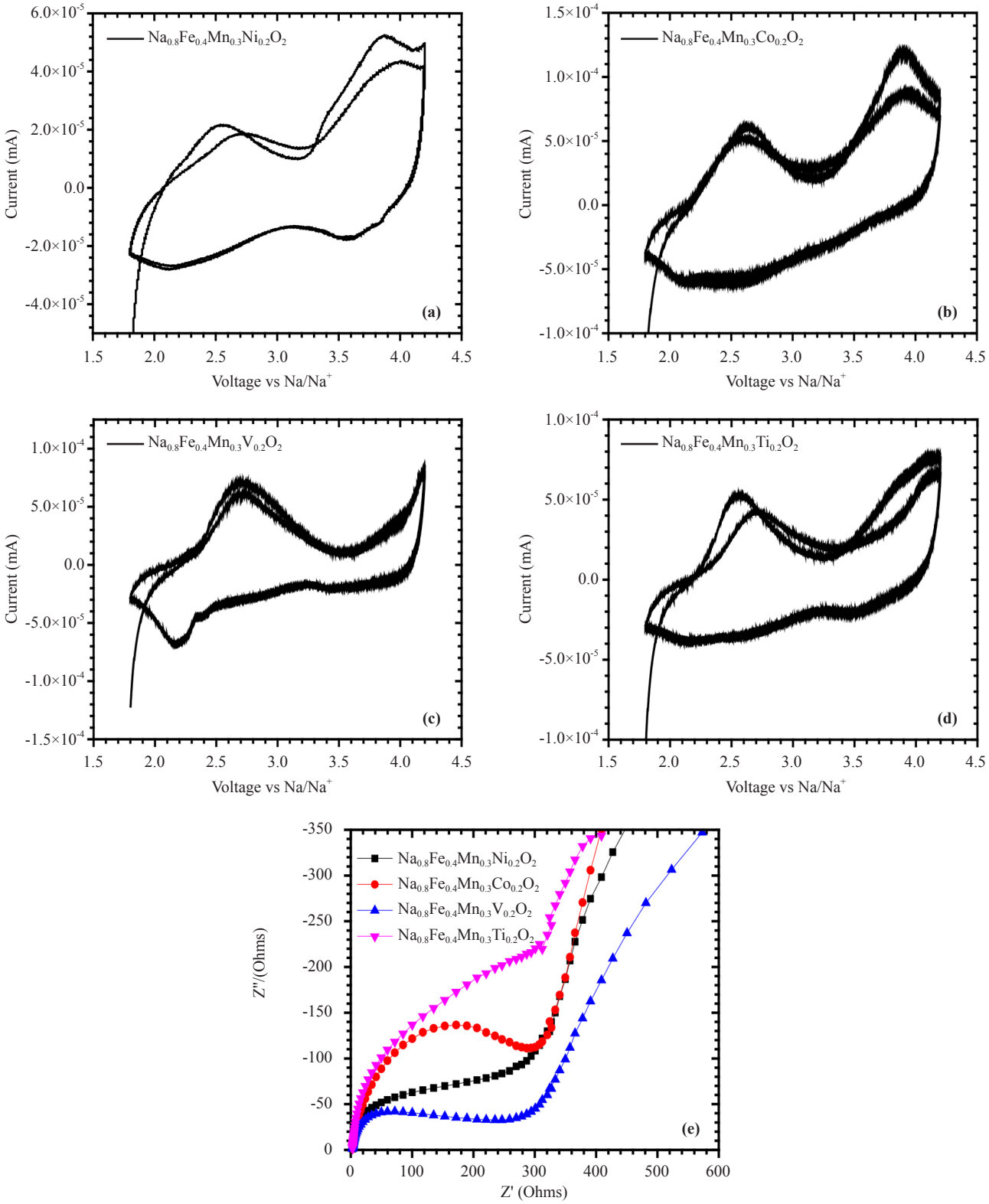


**Figure 5.** Correspondingorresponding cyclic voltammograms analysis of two selected cyclic sweeps of the synthesized samples containing $Na_{0.8}Fe_{0.4}Mn_{0.3}Ni_{0.2}O_2$ (a), $Na_{0.8}Fe_{0.4}Mn_{0.3}V_{0.2}O_2$ (b), $Na_{0.9}Fe_{0.4}Mn_{0.3}Co_{0.2}O_2$ (c), $Na_{0.8}Fe_{0.4}Mn_{0.3}Ti_{0.2}O_2$ (d) as cathode material, and Nyquist plot of EIS data (e)

We choose further to investigate the closely related compositions of our prepared best performing sample $Na_{0.8}Fe_{0.4}Mn_{0.3}Co_{0.2}O_2$ to ascertain other combinations by varying Co and Fe content to $Na_{0.8}Fe_{0.3}Mn_{0.3}Co_{0.3}O_2$, $Na_{0.8}Fe_{0.5}Mn_{0.3}Co_{0.1}O_2$, compounds to clarify electrochemical characterization, stability, morphology and C-rate study. Figure 6 show XRD analysis of the successive combination samples compared with the best sample and all the samples show the same peak positions with O3 crystal structure with space group R3m ($a_{hex}$ = 2.9637 Å; $c_{hex}$ = 16.222 Å), mostly matches with the referenced ICSD85825 and indexed, the 2 theta peak at 41.5° intensity is the highest, containing higher amount of Fe ratio. Figure 7(a, c) shows electrochemical performance and cycle stability test of $Na_{0.8}Fe_{0.3}Mn_{0.3}Co_{0.3}O_2$, $Na_{0.8}Fe_{0.5}Mn_{0.3}Co_{0.1}O_2$, samples analyzed at 2.0-4.2 V with current density of 0.1 C. It is observed that both the samples show different performance efficiencies based solely on the metal content (Fe, Co) ratios as the first and second charge capacities are 98.8 $mAhg^{-1}$, 85.3 $mAhg^{-1}$ and the discharge capacities are 81.5 $mAhg^{-1}$, 74.8 $mAhg^{-1}$ with retention time in first and 90$^{th}$ discharge of 64.6% and charge capacities of the first and second are 146.6 $mAhg^{-1}$, 131.6 $mAhg^{-1}$ with discharge capacities of 130 $mAhg^{-1}$, 122.5 $mAhg^{-1}$ which show a retention time in the first and the 90$^{th}$ discharge 50.3%, respectively. It is worthy to note that the increase of the Co content performance is decreased while the decrease of Co, enhanced performances where the $Na_{0.8}Fe_{0.4}Mn_{0.3}Co_{0.2}O_2$ was the best performing cathode in our study. The stability and retention time along with the Coulombic efficiency characteristics were measured and reported in Figure 7 (b, d) of the closely related samples which are inferior to the best sample whereas stable capacity up to 90 cycles and an average of 98.5% of Coulombic efficiency in our best sample ($Na_{0.8}Fe_{0.6}Mn_{0.3}Co_{0.2}O_2$) were observed. The structural stability of samples shows with an increase of Co content, the stability is much lower but with an increase of Fe content, the stability is better, which perhaps attributes to less Jahn-Teller distortion of crystal structures in the presence of $Fe^{3+}$ ion which is low Jahn-Teller active. Moreover, the C-rate of the cobalt-containing cathodes as presented in Figure 5(e) is well elucidated from 0.1 to 5 C, where a better performance of 38 $mAhg^{-1}$ was exhibited by $Na_{0.8}Fe_{0.4}Mn_{0.3}Co_{0.2}O_2$ ternary cathode at 5 C rate while the other closely related ternary samples $Na_{0.8}Fe_{0.3}Mn_{0.3}Co_{0.3}O_2$, $Na_{0.8}Fe_{0.5}Mn_{0.3}Co_{0.1}O_2$, show performances of 19 $mAhg^{-1}$, 5.8 $mAhg^{-1}$ at 5 C, respectively. The Co transition metal led to an increase in the electronic conductivity and high diffusion value in the O3-type layered structure. From the above results, we can confirm that the high capacity, excellent cycling stability, and rate capability of the $Na_{0.8}Fe_{0.4}Mn_{0.3}Co_{0.2}O_2$ electrode were originated from the well-balanced ternary transition metals compositions in O3-type crystal structure. Thus, we can speculate that the excellent electrochemical performances of the $Na_{0.8}Fe_{0.4}Mn_{0.3}Co_{0.2}O_2$ electrode resulted from the synergetic effects of (i) the high discharge capacity by Fe composition and (ii) structural stabilization via prevention of Fe migration by Co substitution. Moreover, compared to previous work on Fe-based quaternary O3-type layered oxide cathodes [11], our $Na_{0.8}Fe_{0.4}Mn_{0.3}Co_{0.2}O_2$ cathode can achieve a better capacity, rate capability up to 5 C-rate.

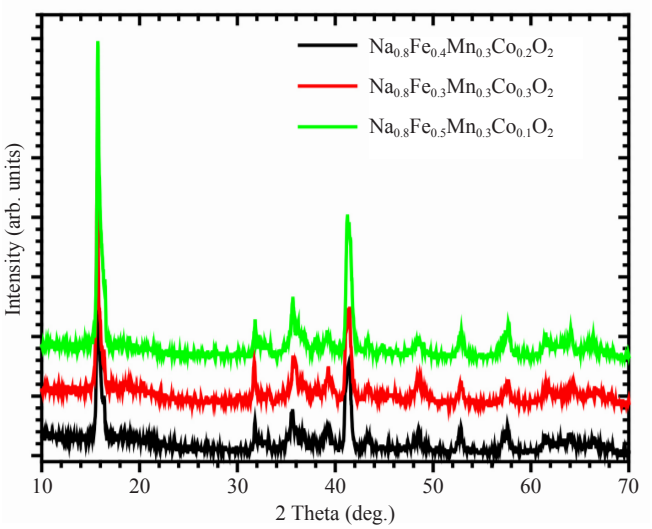


**Figure 6.** X-ray diffraction patterns of O3-type crystal structure with the optimized cobalt content in the ternary cathode materials.

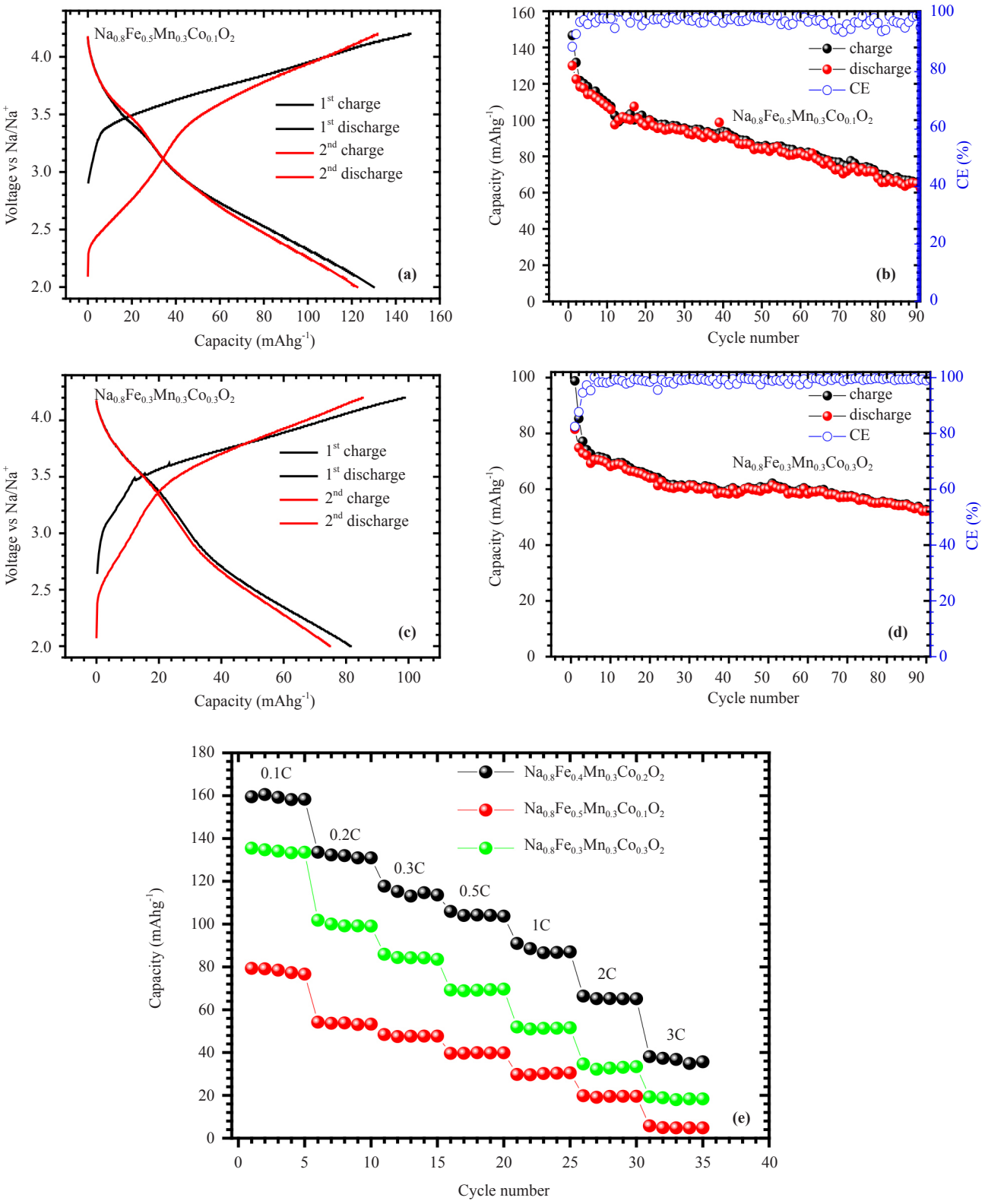


**Figure 7.** Galvanostatic voltage profiles and stability of the optimized samples (a-d) containing O3-type crystal structure in ternary cathode materials. Specific C-rate discharge capacity of the best sample and optimized cobalt content at various rates of 0.1C, 0.2C, 0.5C, 1C, 2C and 5C at ambient (e).

## 4. Conclusion

The well-balanced ternary transition metal structure of O3-type $Na_{0.8}Fe_{0.4}Mn_{0.3}Co_{0.2}O_2$ cathode material was successfully synthesized using the solid-state reaction method. The higher performance of the first and second charge capacities of 162 $mAhg^{-1}$, 170 $mAhg^{-1}$ and discharge capacities of 157 $mAhg^{-1}$, 154 $mAhg^{-1}$, respectively, were observed in the best sample. The existence of high Co metal in the structure resulted in a slight decrease in the discharge capacity. The precise dose of transition metals in the cathode results in enhancing the structural stability and improving the overall cycling stability up to the 90 cycles with 98.5% of Coulombic efficiency exhibiting capacity retention of 82.3% in our best sample. Our results expect a good guide for layered cathode stoichiometric combinations using various transition metals for further development of high-performing positive cathodes for sodium-ion batteries.

## Conflict of interest statement

The authors declare no competing financial interests.

## Acknowledgement

M. A. Khan was grateful to Dongguk University Seoul campus for selecting him a faculty position.

## References

[1] Hwang JY, Myung ST, Sun YK. Sodium-ion batteries: Present and future. *Chemical Society Reviews*. 2017; 46: 3529-3614. Available from: https://doi.org/10.1039/C6CS00776G.

[2] Kim SW, Seo DH, Ma X, Ceder G, Kang K. Electrode materials for rechargeable sodium-ion batteries: Potential alternatives to current lithium-ion batteries. *Advanced Energy Materials*. 2012; 2(7): 710-721. Available from: https://doi.org/10.1002/aenm.201200026.

[3] Mearns E. *Lithium: Reserves, Use, Future Demand and Price*. Energy Matters. 2017. Available from: http://euanmearns.com/lithium-reserves-use-future-demand-and-price/[Accessed January 2018].

[4] Ciez RE, Whitacre JF. The cost of lithium is unlikely to upend the price of Li-ion system. *Journal of Power Sources*. 2016; 320: 310-313. Available from: https://doi.org/10.1016/j.jpowsour.2016.04.073.

[5] BP. *Statistical Review of World Energy*. 2016. Available from: https://www.bp.com/en/global/corporate/energy-economics/statistical-review-of-world-energy.html [Accessed 8 June 2016].

[6] Hueso KB, Armand M, Rojo T. High temperature sodium batteries: status, challenges and future trends. *Energy & Environmental Science*. 2013; 6: 734-749. Available from: https://doi.org/10.1039/C3EE24086J.

[7] Vaalma C, Buchholz D, Weil M, Passerini S. A cost and resource analysis of sodium-ion batteries. *Nature Review Materials*. 2018; 3: 18013. Available from: https://doi.org/10.1038/natrevmats.2018.13.

[8] Yabuuchi N, Kubota K, Dahbi M, Komaba S. Research development on sodium-ion batteries. *Chemical Reviews*. 2014; 114: 11636-11682. Available from: https://doi.org/10.1021/cr500192f.

[9] Kubota K, Komaba S. Review-practical issues and future prospective for Na ion batteries. *Journal of Electrochemical Society*. 2015; 162: A2538-A2550. Available from: https://iopscience.iop.org/article/10.1149/2.0151514jes.

[10] Delmas C, Fouassier C, Hagenmuller P. Structural classification and properties of the layered oxides. *Physica B + C*. 1980; 99: 81-85. Available from: https://doi.org/10.1016/0378-4363(80)90214-4.

[11] Thorne JS, Dunlap RA, Obrovac MN. Structure and electrochemistry of $Na_xFe_xMn_{1-x}O_2$ ($1.0 \leq x \leq 0.5$) for Na ion battery positive electrodes. *Journal of Electrochemical Society*. 2012; 160: A361-A367. Available from: https://doi.org/10.1149/2.058302jes.

[12] Olszewski W, Perez MA, Marini C, Paris E, Wang X, Iwao T, et al. Temperature dependent local structure of $Na_xCoO_2$ cathode material for rechargeable sodium-ion batteries. *Journal of Physical Chemistry C*. 2016; 120: 4227-4232. Available from: https://doi.org/10.1021/acs.jpcc.5b10885.

[13] Li ZY, Zhang J, Gao R, Zhang H, Zheng L, Hu Z, et al. Li-substituted Co-free layered P2/O3 biphasic $Na_{0.67}Mn_{0.55}Ni_{0.25}Ti_{0.2-x}Li_xO_2$ as high-rate-capability cathode materials for sodium ion batteries. *Journal of Physical*

*Chemistry C*. 2016; 120: 9007-9016. Available from: https://doi.org/10.1021/acs.jpcc.5b11983.
[14] Ma X, Chen H, Ceder G. Electrochemical properties of monoclinic $NaMnO_2$. *Journal of the Electrochemistry Society*. 2011; 158: A1307-A1312. Available from: https://iopscience.iop.org/article/10.1149/2.035112jes.
[15] Xiao Y, Zhu YF, Li L, Wang PF, Zhang W, Li C, et al. Structural insights into the dynamic and controlled multiphase evolution of layered-spinel heterostructured sodium oxide cathode. *Cell Reports Physical Science*. 2021; 2: 100547. Available from: https://doi.org/10.1016/j.xcrp.2021.100547.
[16] Yabuuchi N, Kajiyama M, Iwatate J, Nishikawa H, Hitomi S, Okuyama R, et al. P2-type $Na_x[Fe_{1/2}Mn_{1/2}]O_2$ made from earth-abundant elements for rechargeable Na batteries. *Nature Materials*. 2012; 11: 512-517. Available from: https://www.nature.com/articles/nmat3309.
[17] Yabuuchi N, Yoshida H, Komaba S. Crystal structures and electrode performance of alpha-$NaFeO_2$ for rechargeable sodium batteries. *Electrochemistry*. 2012; 80: 716-719. Available from: https://doi.org/10.5796/electrochemistry.80.716.
[18] Yoshida H, Yabuuchi N, Komaba S. $NaFe_{0.5}Co_{0.5}O_2$ as high energy and power positive electrode for sodium-ion batteries. *Electrochemistry Communications*. 2013; 34: 60-63. Available from: https://doi.org/10.1016/j.elecom.2013.05.012.
[19] Yabuuchi N, Yano M, Yoshida H, Kuze S, Komaba S. Synthesis and electrode performance of O3-type $NaFeO_2$-$NaNi_{1/2}Mn_{1/2}O_2$ solid solution for rechargeable sodium batteries. *Journal of the Electrochemistry Society*. 2013; 160: A3131-A3137. Available from: iopscience.iop.org/article/10.1149/2.018305jes.
[20] Oh SM, Myung ST, Hwang JY, Scrosati B, Amine K, Sun YK. High capacity O3-type $Na[Li_{0.05}(Ni_{0.25}Fe_{0.25}Mn_{0.5})_{0.95}]O_2$ cathode for sodium ion batteries. *Chemistry of Materials*. 2014; 26: 6165-6171. Available from: https://doi.org/10.1021/cm502481b.
[21] Yuan D, Hu X, Qian J, Pei F, Wu F, Mao R, et al. P2-type $Na_{0.67}Mn_{0.65}Fe_{0.2}Ni_{0.15}O_2$ cathode material with high-capacity for sodium-ion battery. *Electrochimica Acta*. 2014; 116: 300-305. Available from: https://doi.org/10.1016/j.electacta.2013.10.211.
[22] Guo S, Liu P, Yu H, Zhu Y, Chen M, Ishida M, et al. A layered P2- and O3-type composite as a high-energy cathode for rechargeable sodium-ion batteries. *Angewandte Chemie International Edition*. 2015; 54: 5894-5899. Available from: https://doi.org/10.1002/anie.201411788.
[23] Khan MA, Han DW, Lee GH, Kim II, Kang YM. P2/O3 phase-integrated $Na_{0.7}MnO_2$ cathode materials for sodium-ion rechargeable batteries. *Journal of Alloys and Compounds*. 2019; 771: 987-993. Available from: https://doi.org/10.1016/j.jallcom.2018.09.033.
[24] Hwang JY, Yoon CS, Belharouak I, Sun YK. A comprehensive study of the role of transition metals in O3-type layered $Na[Ni_xCo_yMn_z]O_2$ (x = 1/3, 0.5, 0.6, and 0.8) cathodes for sodium-ion batteries. *Journal of Materials Chemistry A*. 2016; 4: 17952-17959. Available from: https://doi.org/10.1039/c6ta07392a.
[25] Zhao J, Xu J, Lee DH, Dimov N, Meng YS, Okada S. Electrochemical and thermal properties of P2-type $Na_{2/3}Fe_{1/3}Mn_{2/3}O_2$ for Na-ion batteries. *Journal of Power Sources*. 2014; 264: 235-239. Available from: https://doi.org/10.1016/j.jpowsour.2014.04.048.
[26] Li ZY, Zhang J, Gao R, Zhang H, Hu Z, Liu X. Unveiling the role of Co in improving the high-rate capability and cycling performance of layered $Na_{0.7}Mn_{0.7}Ni_{0.3-x}Co_xO_2$ cathode materials for sodium-ion batteries. *ACS Applied Materials Interfaces*. 2016; 8: 15439-15448. Available from: https://doi.org/10.1021/acsami.6b04073.
[27] Jiang X, Hu F, Zhang J. Sodium-deficient O3-$Na_{0.9}Mn_{0.4}Fe_{0.5}Ti_{0.1}O_2$ as cathode material for sodium-ion batteries. *RSC Advances*. 2016; 6: 103238-103241. Available from: https://doi.org/10.1039/C6RA22818F.
[28] Yabuuchi N, Yano M, Yoshida H, Kuze S, Komaba S. Synthesis and electrode performance of O3-type $NaFeO_2$-$NaNi_{1/2}Mn_{1/2}O_2$ solid solution for rechargeable sodium batteries. *Journal of The Electrochemical Society*. 2013; 160(5): A3131-A3137. Available from: https://doi.org/10.1149/2.018305jes..
[29] Barker MG, Hooper AJ. Reactions of sodium oxide with the oxides $VO_2$, $V_2O_3$, VO and vanadium metal. *Chemischer Informationsdienst*. 1973; 4(41): 1066. Available from: https://doi.org/10.1002/chin.197341066.
[30] Chamberland BL, Porter K. A study on the preparation and physical property determination of $NaVO_2$. *Journal of Solid State Chemistry*. 1988; 73: 398-404. Available from: https://doi.org/10.1016/0022-4596(88)90124-7.
[31] Yuan D, Hu X, Qian J, Pei F, Wu F, Mao R, et al. P2-type $Na_{0.67}Mn_{0.65}Fe_{0.2}Ni_{0.15}O_2$ cathode material with high-capacity for sodium-ion battery. *Electrochimica Acta*. 2014; 116: 300-305. Available from: https://doi.org/10.1016/j.electacta.2013.10.211.